Since January 2020 Elsevier has created a COVID-19 resource centre with free information in English and Mandarin on the novel coronavirus COVID-19. The COVID-19 resource centre is hosted on Elsevier Connect, the company's public news and information website.

Cell

Insulin Degrading Enzyme Is a Cellular Receptor Mediating Varicella-Zoster Virus Infection and Cell-to-Cell Spread

Qingxue Li,[1] Mir A. Ali,[1] and Jeffrey I. Cohen[1,*]
[1] Medical Virology Section, Laboratory of Clinical Infectious Diseases, National Institutes of Health, Bethesda, MD, 20892 USA
*Contact: jcohen@niaid.nih.gov
DOI 10.1016/j.cell.2006.08.046

SUMMARY

Varicella-zoster virus (VZV) causes chickenpox and shingles. While varicella is likely spread as cell-free virus to susceptible hosts, the virus is transmitted by cell-to-cell spread in the body and in vitro. Since VZV glycoprotein E (gE) is essential for virus infection, we postulated that gE binds to a cellular receptor. We found that insulin-degrading enzyme (IDE) interacts with gE through its extracellular domain. Downregulation of IDE by siRNA, or blocking of IDE with antibody, with soluble IDE protein extracted from liver, or with bacitracin inhibited VZV infection. Cell-to-cell spread of virus was also impaired by blocking IDE. Transfection of cell lines impaired for VZV infection with a plasmid expressing human IDE resulted in increased entry and enhanced infection with cell-free and cell-associated virus. These studies indicate that IDE is a cellular receptor for both cell-free and cell-associated VZV.

INTRODUCTION

Varicella-zoster virus (VZV) is the etiologic agent of varicella (chickenpox) and zoster (shingles). VZV is a member of the α-herpesvirus family and is closely related to the other two human virus members of the family, herpes simplex virus (HSV) 1 and 2. Acute infection with VZV is followed by cell-associated viremia and the rash of varicella (Arvin, 2001). The virus establishes latency in the nervous system and can reactivate to cause zoster. While varicella is likely transmitted by cell-free airborne virions, in cell culture VZV is highly cell associated, and the virus is propagated by cell-to-cell spread with no infectious virus present in the medium. The virus is thought to spread within the body by cell-to-cell transfer of virus.

The mechanism of VZV entry into target cells and spread from cell-to-cell is not well understood. Previous studies showed that VZV, like other members of the herpesvirus family, engages cell surface heparan sulfate for initial attachment (Zhu et al., 1995). Mannose 6-phosphate inhibits infection with cell-free VZV, which implicates the cation-independent mannose 6-phosphate receptor (MPR^{ci}) in facilitating entry of cell-free virus by interacting with viral glycoproteins that contain phosphorylated N-linked complex oligosaccharides (Gabel et al., 1989; Zhu et al., 1995). Chen et al. (2004) used stable cell lines deficient in MPR^{ci} to show that the protein is required for infection by cell-free VZV (Chen et al., 2004). However, soluble MPR^{ci} did not bind to viral glycoproteins in ligand-blotting assays (Zhu et al., 1995). Cell lines deficient in MPR^{ci} are not impaired for infection by cell-associated virus; thus, MPR^{ci} is not a cellular receptor for cell-to-cell spread of the virus.

Studies of HSV-1 and HSV-2 have identified viral and/or cellular proteins required for entry and cell-to-cell spread. Herpes virus entry mediator A, nectin-1 and nectin-2, and 3-O-sulfated heparan sulfate have each been established as HSV receptors for entry of cell-free virus (Cocchi et al., 1998; Geraghty et al., 1998; Montgomery et al., 1996; Shukla et al., 1999). HSV glycoprotein D (gD) has been identified as the viral ligand for each of these receptors. HSV gE/gI, though not essential for entry and replication, sorts nascent virions to cell junctions and is required for efficient cell-to-cell spread of HSV (Collins and Johnson, 2003; Dingwell and Johnson, 1998). Although a cellular receptor for gE/gI has been postulated, it has not yet been identified.

VZV encodes at least seven glycoproteins, gB, gC, gE, gH, gI, gK, gL, all of which have well-conserved homologs in HSV (Cohen and Straus, 2001). In contrast to HSV, VZV does not have a homolog for gD. While HSV gD is one of five glycoproteins in the unique short region of its genome, the corresponding portion of VZV encodes only two VZV glycoproteins, gE and its chaperon gI. Since HSV gD is the receptor binding protein for HSV, and VZV gI is not required for infection by VZV (Cohen and Nguyen, 1997), VZV gE might be important for binding to a cellular receptor. HSV gE or HSV gD alone do not mediate membrane fusion. The minimum requirement for HSV fusion to cells is the coexpression of four glycoproteins (gD, gB, gH, and gL) and a cell-surface entry receptor specific for gD

(Pertel et al., 2001). Syncytia formation in VZV, a hallmark of cell-to-cell spread, is due to fusion of cell membranes mediated by gH and gL, or gB and gE (Cole and Grose, 2003). While expression of gH or gB alone induce a modest amount of fusion, expression of gE alone is not sufficient for fusion unless it is coexpressed with gB (Maresova et al., 2001). Attempts to generate a VZV gE deletion mutant were unsuccessful (Mo et al., 2002), and a gE minus virus could only be constructed using cells expressing gE (Q.L. and J.C., unpublished data). Taken together, these findings indicate that VZV gE is an essential glycoprotein for VZV. Antibodies to gE neutralize virus in vitro, and immunization with a vector expressing gE protects animals from challenge with virus (Lowry et al., 1992; Wu and Forghani, 1997). Therefore, VZV gE may be involved in viral entry and cell-to-cell spread and is a likely candidate for binding to a cellular receptor.

In this study we identified insulin-degrading enzyme (IDE) as a cellular receptor for gE. IDE forms a complex with both the purified extracellular domain and the native form of gE in VZV-infected cells. Inhibition of IDE results in reduced VZV infectivity and cell-to-cell spread. Expression of human IDE in nonhuman cell lines that are impaired for VZV infection enhanced virus infection, entry, and binding. These experiments identify IDE as a VZV receptor and confirm the essential role that gE plays in VZV infection.

RESULTS

The Extracellular Domain of gE Interacts with IDE

VZV gE is essential for virus replication and may be important for virus entry. To identify cellular ligands that interact with gE, a soluble form of the extracellular domain of gE fused to human Ig Fc was immobilized on protein A-Sepharose beads and used in a pull-down assay with cell lysates from human melanoma cells that are permissive for VZV infection. After extensive washing, the bound proteins were resolved on SDS-PAGE gels and stained with Coomassie blue. A unique band of about 120 kDa (Figure 1A) was pulled down by the gE-Fc fusion protein but was absent from protein lysates incubated with Sepharose alone or control Fc fusion proteins. The band was excised, and sequencing identified the protein as IDE.

To confirm the interaction of gE with IDE and rule out the possibility of binding to the Fc tag, pull-down assays were performed using truncated gE without an Fc tag (gEt) immobilized onto protein A-Sepharose beads with monoclonal antibody to gE and incubated with lysates from HeLa cells or human T cells. After extensive washing, the beads were boiled in sample buffer, subjected to SDS-PAGE separation, transferred to membranes, and immunoblotted with polyclonal anti-IDE antibody. gEt formed a complex with IDE that was detected with antibody to gE in both HeLa and T cells (Figure 1B, lanes 5–6) but not in HeLa cells when a control antibody was used in place of antibody to gE (Figure 1B, lane 4). IDE also bound to gE in VZV-infected melanoma cells. Immunoprecipitation of gE with anti-gE antibody followed by immunoblotting with anti-IDE antibody indicated that gE interacted with IDE in VZV-infected but not uninfected cells (Figure 1B, lanes 1–3).

gB and gH play important roles in viral entry and/or infectivity of herpesviruses. We tested whether IDE interacts with VZV gB, VZV gH, VZV gI, or HSV gE. Lysates from VZV-infected cells were immunoprecipitated with antibodies to VZV gE, gB, or gH and immunoblotted with anti-IDE antibody. While gE coimmunoprecipitated with IDE, gB and gH did not interact with IDE (Figure 1C, lanes 7–9). Transfection of CV-1 cells with plasmids expressing VZV gE, VZV gI, or HSV gE followed by immunoprecipitation with the corresponding antibody and immunoblotting with anti-IDE antibody showed that the extracellular domain of VZV gI, which functions as a gE chaperone but lacks sequence homology with gE, also interacted with IDE, although at a much weaker level than gE (Figure 1C, lanes 1 and 2). This was confirmed using an ELISA-based ligand binding assay. When similar levels of His-tagged soluble gE, gI, or gB were incubated with HA-IDE, the latter bound significantly greater to gE than to either gB or gI over a range of concentrations (Figure 1D). HSV gE, which has 32% amino acid identity with VZV gE within a 170 amino acid region, interacted very weakly with IDE (Figure 1C, lane 4).

Immunoprecipitation of IDE from infected cells followed by immunoblotting with antibody to gE showed that the amount of gE-IDE complexes increased during the course of VZV infection (Figure S3), which was in parallel with the increasing amounts of gE produced in these infected cells over time, even though the total amount of IDE remained unchanged (data not shown).

A Portion of IDE that Interacts with gE Is Located on the Plasma Membrane

Computer analysis indicates that the predicted sequence of IDE contains a putative amino-terminal signal peptide with a potential cleavage site between residues 22 and 23, and the majority of the sequence might be extracellular; however, a typical transmembrane domain is not apparent (TMHMM program, Technical University of Denmark). Cell fractionation studies showed that IDE is localized primarily in the cytosol (Akiyama et al., 1988), with a small amount present on the cell-surface plasma membrane (Seta and Roth, 1997; Yaso et al., 1987). Vekrellis et al. (2000) identified a ~115 kDa cell-surface membrane-associated IDE isoform on neuronal cells (Vekrellis et al., 2000). To verify that IDE is present on the surface of cells, we biotinylated cell surface proteins followed by immunoprecipitation with streptavadin-coated agarose beads and immunoblotting with anti-IDE antibody. A protein of ~120 kDa was present on the surface of HeLa and melanoma cells (Figure 2A, lanes 1 and 2).

To determine whether gE interacts with IDE on the plasma membrane, cell-surface proteins were biotinylated and incubated with gEt. The IDE-gE complex was immunoprecipitated with gE antibody followed by

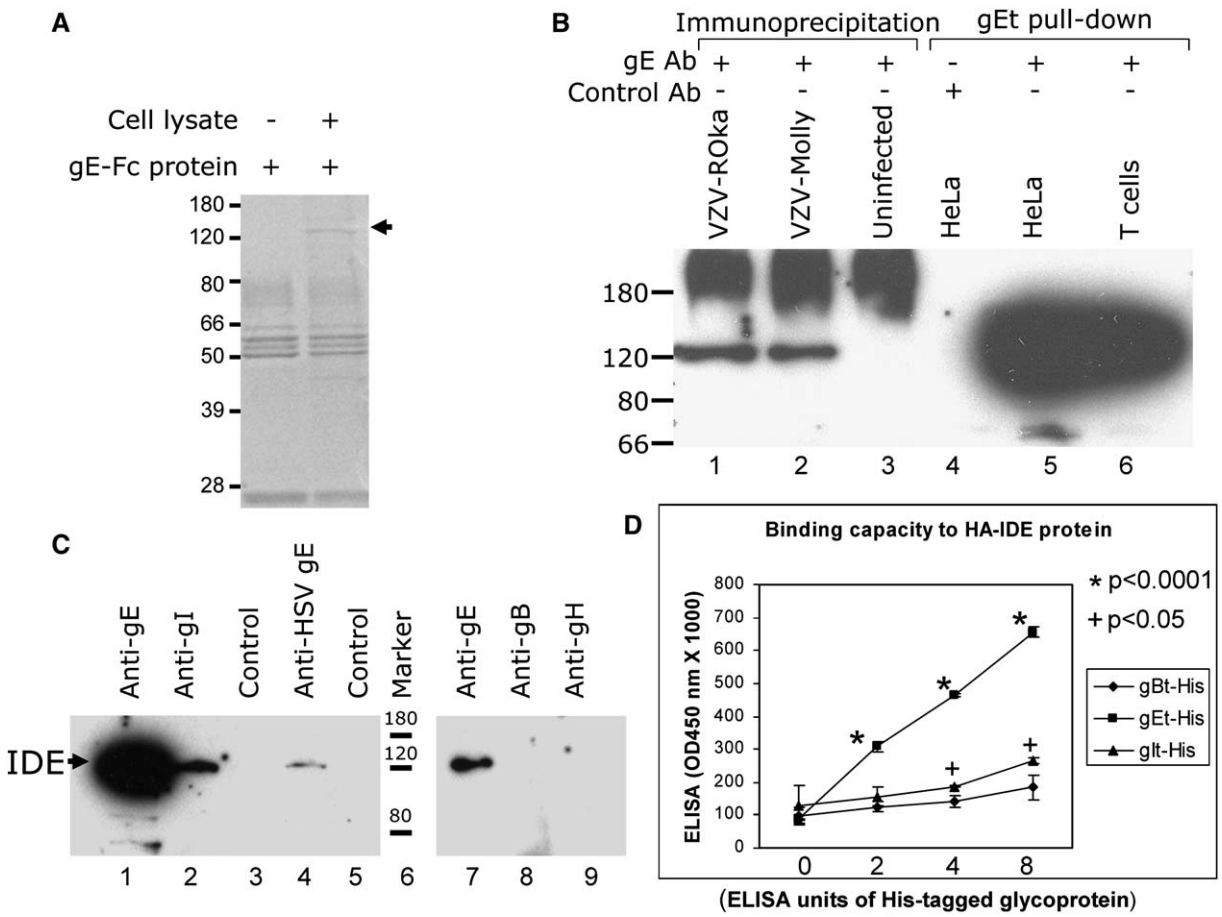

Figure 1. IDE Interacts with the Extracellular Domain of VZV gE but Not gB or gH

(A) The extracellular domain of gE fused to the Fc portion of human IgG (gE-Fc) bound to protein-A Sepharose was incubated with a cell lysate from melanoma cells, and proteins that bound to gE-Fc were resolved on SDS-PAGE and stained with Coomassie blue. A 120 kDa cellular protein is present in the cell lysate that interacts with gE-Fc.

(B) gE protein from VZV ROka-infected cells (lane 1) or VZV Molly, a low-passage clinical isolate (lane 2), was immunoprecipitated with monoclonal anti-gE antibody, and IDE was detected in immune complexes. Purified extracellular domain of gE (gEt) immobilized onto protein-A Sepharose beads with anti-gE antibody (lanes 5 and 6) pulls down IDE from cell lysates.

(C) Plasmids encoding the extracellular domain of VZV gE (lane 1), gI (lane 2), full-length HSV gE (lane 4), or control vectors (lanes 3 and 5) were transfected into CV-1 cells, and immunoprecipitation with the respective antibodies pull down IDE with VZV gE and, to a lesser extent, with gI. Lysates from VZV-infected cells immunoprecipitated with anti-gE, but not with anti-gB or anti-gH, antibody pull down IDE (lanes 7–9).

(D) ELISA plates were coated with HA-IDE and incubated with equal amounts of His-tagged gEt, gBt, or glt, and binding was assayed using anti-His antibody. HA-IDE binds to gEt significantly greater than to glt or gBt. Error bars show standard deviations, and t test was used to determine p values.

immunoblotting with streptavidin-conjugated HRP to detect cell surface IDE or anti-IDE antibody to detect total IDE. A portion of the total IDE in the gE-IDE complex was derived from IDE on the cell surface (Figure 2B, lanes 2 and 6). Controls lacking antibody to gE showed that the IDE-gE interaction was required for detection of IDE on the cell surface in this assay (Figure 2B, lanes 3 and 4).

Anti-IDE Antibodies and Soluble IDE Extracted from Liver Reduce VZV Infectivity and Cell-to-Cell Spread

Polyclonal and monoclonal IDE antibodies were tested for their ability to block VZV infection. Commercially available polyclonal anti-IDE antibody PRB-282C and monoclonal antibody 9B12 (Covance, Berkeley, CA) were used. In several experiments, addition of either antibody (50 ug/ml for 9B12 and 1/200 dilution for PRB-282C serum) to MeWo cells prior to VZV infection resulted in 30%–45% inhibition of virus infectivity (Figures 3A and 3B), while a control antibody (anti-CD3) or normal rabbit serum showed little or no effect. Polyclonal antibody (Figure S4) blocked VZV infection in a dose-dependent manner.

To determine if IDE antibody affects cell-to-cell spread of VZV, we preincubated cells with the polyclonal antibody at 1/100 to 1/200 dilutions at 4°C for 60 min followed by infection with cell-free ROka-lacZ in the presence of the antibody. Three days later the cells were stained with X-gal. IDE antibody markedly reduced plaque sizes compared to the cells treated with control normal rabbit serum

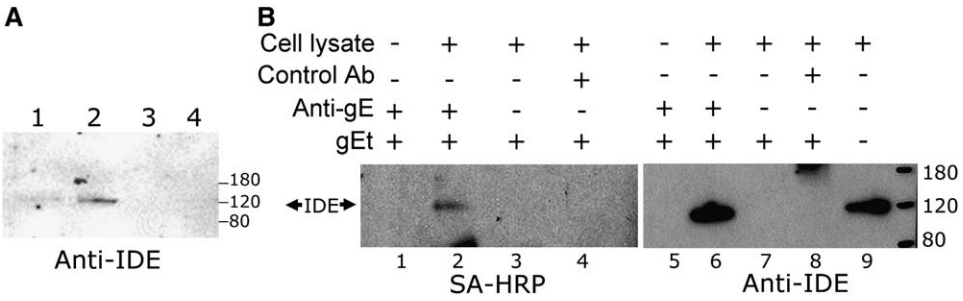

Figure 2. The Extracellular Domain of gE Interacts with IDE on the Surface of Cells

(A) Biotinylated cell-surface proteins that were precipitated with streptavidin-coated agarose beads pull down IDE from the surface of HeLa (lane 1) or melanoma (lane 2) cells as detected by immunoblotting with antibody to IDE. In the absence of biotinylation, IDE is not detected on the surface of HeLa (lane 3) or melanoma (lane 4) cells.

(B) Monolayers of CV-1/EBNA-1 cells were biotinylated for 30 min at room temperature in PBS to label cell-surface proteins. After extensive washing, the cells were lysed and incubated with soluble gEt that had been immobilized on beads using anti-gE antibody. After washing, the beads were boiled in SDS-protein gel solution, and a 120 kDa protein was detected after blotting with Streptavidin-HRP to detect cell-surface IDE, or with anti-IDE to detect total IDE. Lane 9 represents lysate not incubated with beads.

(Figure 3C). Therefore, IDE antibody inhibits cell-to-cell spread of VZV.

To determine whether purified soluble IDE can inhibit entry of VZV, we incubated cell-free ROka-lacZ with soluble IDE extracted from liver or uninfected sonicated cell protein as a control, at 37°C for 30 min before infection of melanoma cells. Four days postinfection the cells were stained with X-gal and the number of blue foci, indicative of infectivity by cell-free virus, were scored. Soluble IDE inhibited infectivity by ~70%, while control protein had no effect (Figure 3D). In three independent experiments, IDE inhibited VZV infectivity by 50%–70%. In contrast, when soluble IDE was added at 1.5 hr after infection, it failed to reduce the number of VZV foci (data not shown), suggesting that soluble IDE extracted from liver blocks VZV entry during the initial stages of infection.

To determine if soluble IDE extracted from liver affects cell-to-cell spread of VZV, we infected cells with cell-free ROka-lacZ in the presence of soluble IDE or control protein (37.5 μg/ml each) and added the proteins again on the second day of infection. Two days later the cells were stained with X-gal. Soluble IDE markedly reduced plaque sizes compared to the cells treated with control protein or no added protein (Figure 3E). Therefore, soluble IDE inhibits cell-to-cell spread of VZV.

Interestingly, VZV infectivity was enhanced when the virus was pretreated with recombinant soluble IDE (rIDE) produced in a baculovirus expression system (Figure 3F). rIDE is initiated from the second ATG of the IDE coding sequence and thus is missing the first 41 amino acids of the protein. Since rIDE is produced in insect cells, it may be processed differently than IDE extracted from liver. The enhancement of VZV infectivity by rIDE supports a role for IDE in an early stage of VZV infection. Several soluble receptor molecules have been described that can either block or promote virus infection, including nectin-1 for HSV (Kwon et al., 2006; Lopez et al., 2001) and sCD4 for HIV (Sattentau and Moore, 1991; Smith et al., 1987).

Since IDE interacts with gE, and IDE degrades several proteins, including insulin (Farris et al., 2003; Goldfine et al., 1984) and amylin (Farris et al., 2003; Vekrellis et al., 2000), we determined whether IDE degrades gE. Incubation of purified IDE with gEt at 37°C for 4 hr did not reduce the amount of the glycoprotein, while IDE degraded insulin when incubated at 37°C for 30 min (Figure S1A). Conversely, addition of bacitracin (1 mg/ml), an IDE inhibitor that reduces degradation of insulin and amylin by IDE (Bennett et al., 2003), did not change the turnover rate of gE in VZV-infected cells during a pulse-chase experiment (Figure S1B). These results suggest that IDE is not important for degradation of gE in cells.

Knockdown of IDE Expression Inhibits VZV Infection and Cell-to-Cell Spread

To determine the role of IDE in VZV infection, we used small interfering RNA (siRNA) to reduce endogenous IDE expression. Human fibroblasts (MRC-5 cells) that are susceptible to productive VZV infection were transfected with two independent pools of IDE-specific siRNAs (siRNA-IDE1, siRNA-IDE2) or two independent control siRNA pools (siRNA-1, siRNA-2). At 2.5 days after transfection, half of the cells were harvested for immunoblotting to determine the level of IDE, and the remainder of the cells was infected with cell-free ROka-lacZ. IDE-specific siRNA knocked down the IDE level by about 95% compared with control siRNAs, as calculated by densitometry (Figure 4A). To determine the effect of IDE knockdown on VZV infection, the cells infected with cell-free ROka-lacZ were stained with X-gal 4 days later. VZV infectivity in the cells transfected with IDE-specific siRNA was reduced by about 70% compared with the cells transfected with control siRNA (Figure 4B). Interestingly, most of the X-gal positive foci in the cells transfected with IDE-specific siRNA consisted of only single isolated blue cells (Figure 4C, panels 3 and 4); in contrast, larger foci involving multiple cells, due to cell-to-cell spread of virus, were

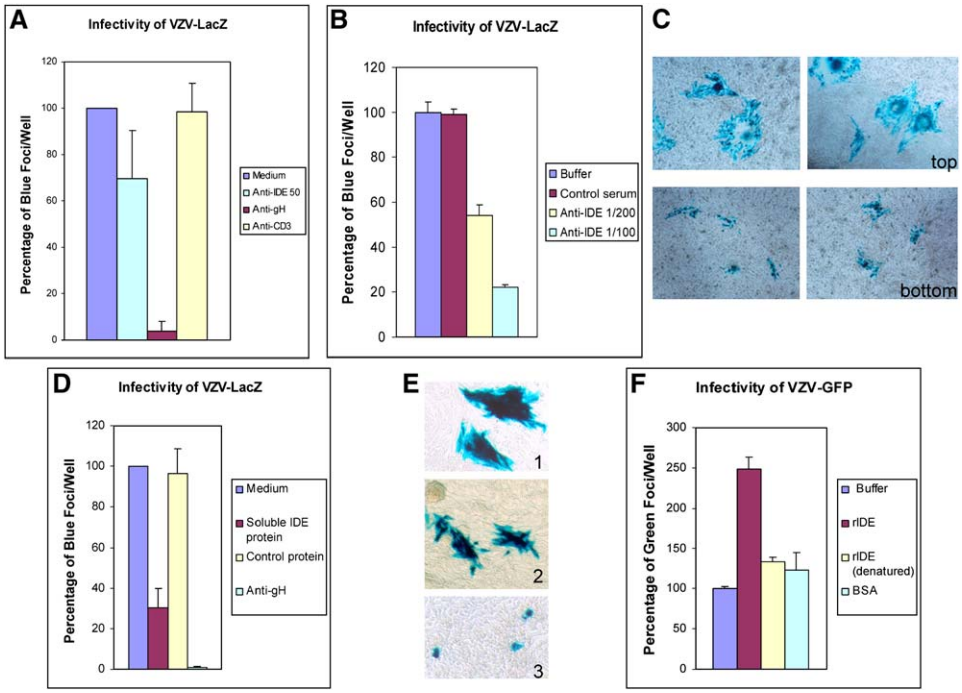

Figure 3. Anti-IDE Antibodies and Soluble IDE Extracted from Liver Reduce VZV Infectivity and Virus Cell-to-Cell Spread

(A) Monoclonal anti-IDE antibody (50 ug/ml) or anti-gH antibody, but not control anti-CD3 antibody, inhibits the number of foci that stain with X-gal in cells infected with ROka-lacZ. The figure shows the average of two independent experiments; P = 0.002 for anti-IDE antibody compared with medium control.

(B) Polyclonal anti-IDE serum reduces the number of VZV-lacZ foci compared with normal rabbit serum or buffer controls. The figure shows the average of two independent experiments; p = 0.002 for anti-IDE 1/100 versus buffer; p < 0.001 for anti-IDE 1/100 versus preimmune serum.

(C) Plaque sizes are reduced in cells infected with cell-free VZV-lacZ treated with polyclonal anti-IDE serum (bottom panels) compared with cells treated with normal rabbit serum (top panel). Magnification of 40×.

(D) Purified soluble IDE protein extracted from liver (37.5 μg/ml) or anti-gH antibody, but not control soluble protein from uninfected cells, inhibits infectivity in cells infected with cell-free ROka-lacZ. Virus was preincubated with soluble IDE at 37°C for 30 min before infection. Percentage of blue foci is set at 100% for cells infected in the presence of media. P = 0.0004 by ANOVA.

(E) Plaque sizes in cells infected with cell-free VZV-lacZ treated with soluble IDE extracted from liver (3), but not medium (1) or control protein (2), are reduced. Magnification of 100×.

(F) rIDE, but not BSA control or denatured rIDE (by pH 11.5), enhances VZV infectivity. Cell-free VZV-GFP virus was preincubated with rIDE at 20 μg/ml at 37°C for 30 min before infection. Three days postinfection, GFP-positive foci were counted. P < 0.04 for rIDE versus buffer, denatured rIDE, or BSA. The experiment was repeated with similar results. Error bars show standard deviations.

present in the cells transfected with control siRNA (Figure 4C, panels 1 and 2). Knockdown of IDE with siRNA also inhibited infectivity of cell-associated wild-type VZV (Figure 4D). Transfection with IDE-specific siRNA did not reduce cell viability compared with control siRNA.

Bacitracin, which Inhibits IDE, Blocks gE-IDE Complex Formation, VZV Infection, and Cell-to-Cell Spread

Since bacitracin inhibits IDE (Bennett et al., 2003), we examined the effect of the antibiotic on the interaction of gE with IDE, VZV infectivity, and cell-to-cell spread. Bacitracin was incubated with cell lysates in the presence of gEt and immune complexes were immunoprecipitated with anti-gE antibody and probed with antibody to IDE. Bacitracin inhibited gEt-IDE complex formation in a dose-dependent manner (Figure 5A). Bacitracin also inhibited the interaction of IDE with gE-Fc fusion protein (G.L. and J.C., unpublished data). Bacitracin inhibited plaque formation of cell-free VZV ROka-lacZ in a dose-dependent manner with ~90% reduction in infectivity at 5 mg/ml of antibiotic (Figure 5B).

Plaque size in the presence of 1 mg/ml of bacitracin, added either at the time of infection or 8 hr after infection to allow virus entry, was reduced, indicating that the drug also reduced cell-to-cell spread of VZV. This effect was observed in cells infected with either wild-type cell-associated virus (Figure 5C) or with vaccine-derived cell-free virus (Figure 5D). In contrast, bacitracin did not inhibit either infectivity or cell-to-cell spread of HSV-1, but the same dose of antibiotic inhibited cell-to-cell spread and infectivity of VZV (Figure 5E). Bacitracin did not cause apparent cytotoxicity and did not inhibit adenovirus

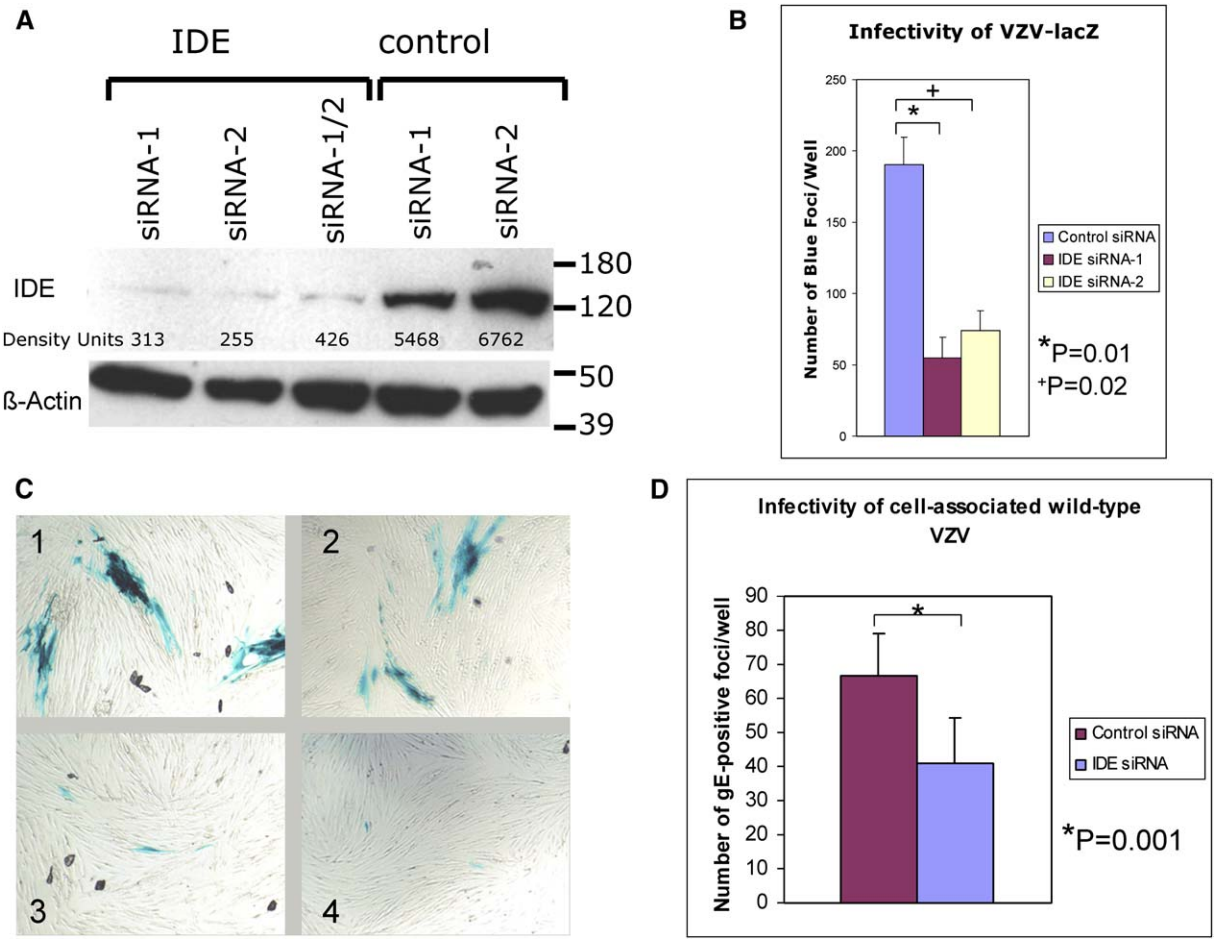

Figure 4. Knockdown of Expression of IDE Blocks VZV Infectivity and Prevents VZV Cell-to-Cell Spread

(A) MRC-5 cells transfected with two independent specific IDE siRNA pools show reduced levels of IDE protein compared with cells transfected with two independent nonspecific control siRNA pools.

(B) MRC-5 cells transfected with IDE siRNA and infected with cell-free ROka-lacZ show reduced numbers of foci that stain with X-gal at 4 days postinfection, compared with cells transfected with control siRNA.

(C) MRC-5 cells transfected with IDE-specific siRNA and infected with cell-free ROka-lacZ (panels 3 and 4) show reduced size of infectious foci at 4 days after infection, compared with cells transfected with control siRNA (panels 1 and 2). Magnification of 100×.

(D) MRC-5 cells were transfected with siRNAs, and, after 2.5 days, the cells were infected with cell-associated wild-type (low-passage, Molly strain) VZV for 1.5 hr and then washed twice to remove the inoculum. The cells were fixed 24 hr after infection, stained with mouse anti-gE antibody, followed by FITC-conjugated anti-mouse antibody, and the number of immunofluorescent foci were counted. The figure represents the results of two independent experiments.

Error bars show standard deviations, and t test was used to determine p values.

infectivity at the doses used (data not shown). Thus, the effect of bacitracin was specific for VZV and was not seen with HSV-1, another human α-herpesvirus.

To ensure that the effects of bacitracin on VZV entry and cell-to-cell spread were not due to an effect on virus replication, we performed electron microscopy on VZV ROka-infected cells in the presence or absence of bacitracin. Bacitracin (1.0 mg/ml) was added to melanoma cells at 8 hr postinfection to allow viral entry. The cells were then incubated for an additional 20 hr. Bacitracin did not reduce nucleocapsid formation, virion maturation, transport to the cell surface, or the number of cell-surface virions when compared with untreated controls (Figure S2). These data indicate that bacitracin did not inhibit VZV replication or trafficking to the cell surface.

Expression of Exogenous Human IDE Increases VZV Infectivity and Entry

To further investigate the function of IDE in VZV infection, we performed a series of gain-of-function experiments. Chinese hamster ovary (CHO) cells, which do not support productive VZV infection, were transiently transfected with either a plasmid expressing HA-tagged human IDE or empty vector and infected with cell-free VZV-GFP virus. This virus encodes GFP under a CMV promoter so that productive infection is not required for expression of

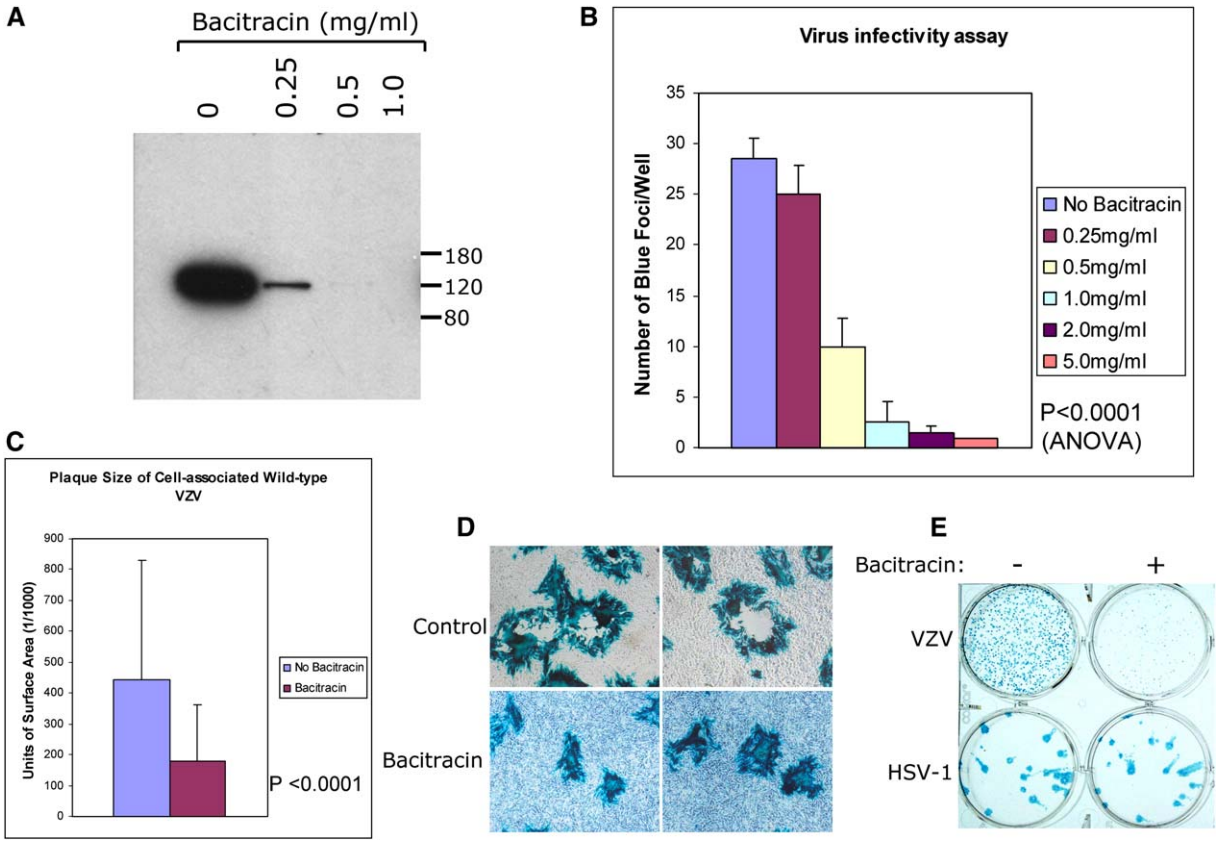

Figure 5. Bacitracin, an IDE Inhibitor, Blocks IDE-gE Complex Formation, Inhibits VZV Infectivity, and Reduces Viral Cell-to-Cell Spread

(A) Bacitracin reduces binding of soluble gE to IDE in a pull-down assay.

(B) Bacitracin reduces the number of X-gal positive foci in melanoma cells infected with cell-free ROka-lacZ 4 days postinfection.

(C) Bacitracin inhibits cell-to-cell spread of cell-associated wild-type VZV. Melanoma cells were infected with cell-associated low passage (Molly strain) VZV in the presence or absence of bacitracin (1.0 mg/ml) for 24 hr. Cells were fixed and plaques stained with anti-gE antibody. Cell-to-cell spread was determined by measuring plaque size of virus-infected cells (Collins and Johnson, 2003). The surface area of photographed plaques in bacitracin-treated (N = 35) and -untreated (N = 51) cells was analyzed by Image J software. P values were calculated using a t test.

(D) Bacitracin reduces the size of plaques for melanoma cells infected with cell-free ROka-lacZ (lower panels, two representative fields), compared to cells infected in the absence of the antibiotic (upper panels, 2 fields). Magnification of 100×.

(E) Bacitracin reduces the number and size of foci in melanoma cells infected with cell-free ROka-lacZ but not HSV-1-LacZ.

Error bars show standard deviations.

GFP. Two days later, cells transfected with human IDE showed a 3-fold increase in infectivity (Figure 6A). A modest amount of virus was able to enter the cells (vector control) in the absence of human IDE, indicating that the cells are not completely defective for entry. Similar results were obtained with mouse melanoma cells (B78H1) infected with VZV (data not shown). Since CHO and mouse melanoma cells do not support productive infection, the ability of human IDE to increase the number of GFP-positive cells after incubation with VZV suggests that the IDE is important for a very early step in virus infection.

To measure entry of VZV into cells, CHO cells that stably express human IDE (B3 cells), or their parental control cell line, were transfected with a reporter plasmid that encodes GFP under a T7 promoter. The CHO cells were then incubated for 18 hr with melanoma cells infected with VZV-encoding T7 polymerase (ROka-T7). Expression of the T7 promoter-driven GFP is turned on in cells infected with ROka-T7. The level of GFP expression was detected by anti-GFP antibody in immunoblot, and the bands were quantified by densitometry. Cells stably expressing IDE showed a 3-fold increase in GFP expression, indicative of enhanced entry when compared with control cells (Figure 6B). A 3-fold increase in GFP expression was also seen when porcine cells (SK-6 A7), which do not support productive VZV infection, cotransfected with the GFP reporter plasmid, and plasmid expressing human IDE or empty vector were used in place of CHO and CHO B3 cells in the assay described above (unpublished data).

To determine whether exogenous expression of human IDE in CHO cells enhances stable binding of VZV to the cells, we transfected CHO cells with a plasmid expressing

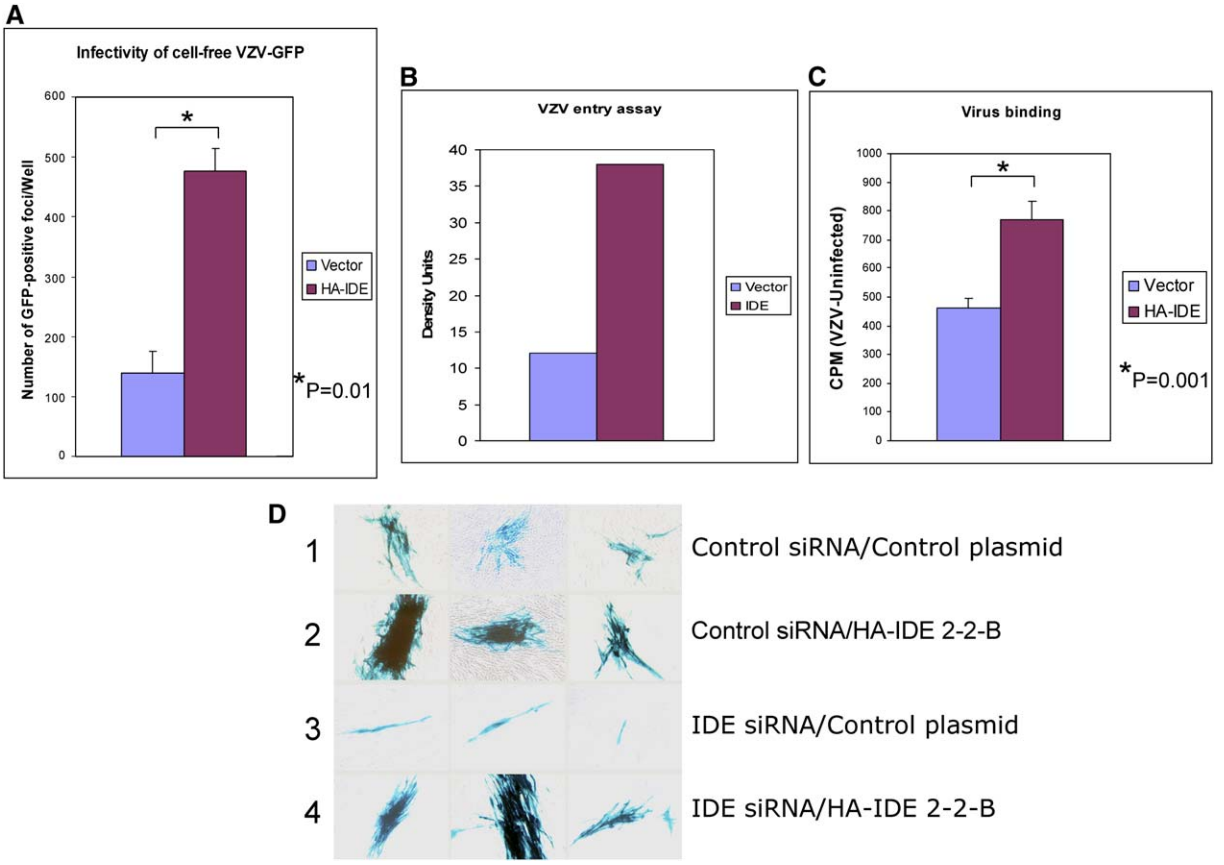

Figure 6. Expression of Exogenous Human IDE Increases VZV Entry and Infectivity and Rescues Impaired VZV Cell-to-Cell Spread that Results from Knockdown of IDE

(A) Transfection of CHO cells with a plasmid encoding HA-tagged human IDE followed by infection with cell-free ROka-GFP increases the number of GFP-positive foci, compared with cells transfected with control plasmid.

(B) Cells stably expressing human IDE show increased GFP by densitometry after transfection with a reporter plasmid that encodes GFP under a T7 promoter and incubation with cell-associated VZV encoding the T7 polymerase (ROka-T7), when compared with a control cell line that does not express human IDE. The result was repeated in three additional experiments using two different cell lines (CHO and SK6-A7), and the range of enhancement of VZV entry by IDE was 2.2- to 12.5-fold.

(C) Transfection of CHO cells with HA-IDE results in increased binding of [^{35}S]methionine labeled cell-free VZV compared with cells transfected with control plasmid. Counts per minute (CPM) were obtained by subtracting those from lysates of uninfected cells from virus-infected cells. The binding assay was performed in the presence of heparin to eliminate the contribution of attachment through cell-surface heparan sulfate. Error bars show standard deviations, and t test was used to determine p values.

(D) Cotransfection of MRC-5 cells with control siRNA and plasmid expressing HA-IDE followed by infection with cell-free ROka-lacZ show increased size of infectious foci (panel 2), compared with cells transfected with control siRNA and control plasmid (panel 1). Cells transfected with IDE-specific siRNA and control plasmid and infected with ROka-lacZ show smaller-sized infectious foci (panel 3) than cells transfected with control siRNA and control plasmid (panel 1). Cells transfected with IDE-specific siRNA and plasmid that expresses HA-IDE that is resistant to the siRNA, followed by infection with ROka-lacZ, show increased size of infectious foci (panel 4), compared to cells transfected with IDE-specific siRNA and control plasmid (panel 3).

Error bars show standard deviations.

HA-tagged human IDE or control plasmid, and 2 days later, the cells were incubated with radiolabeled cell-free VZV in the presence of heparin at 4°C for 1.5 hr to assay for stable binding. Expression of human IDE increased heparin-resistant binding of VZV to CHO cells by ~1.6-fold (Figure 6C). While the ability of exogenous human IDE to increase VZV infectivity and binding was reproducible, the overall effect was somewhat modest. Endogenous IDE in CHO cells may have interfered with expression of exogenous human IDE and obscured the effect or expression of the human protein.

Expression of Exogenous Human IDE Corrects the Defect in Cell-to-Cell Spread in IDE Knockdown Cells

Since IDE knockout cells could not be obtained for gain-of-function experiments, we cotransfected human fibroblasts (MRC-5 cells) with IDE-specific siRNA to

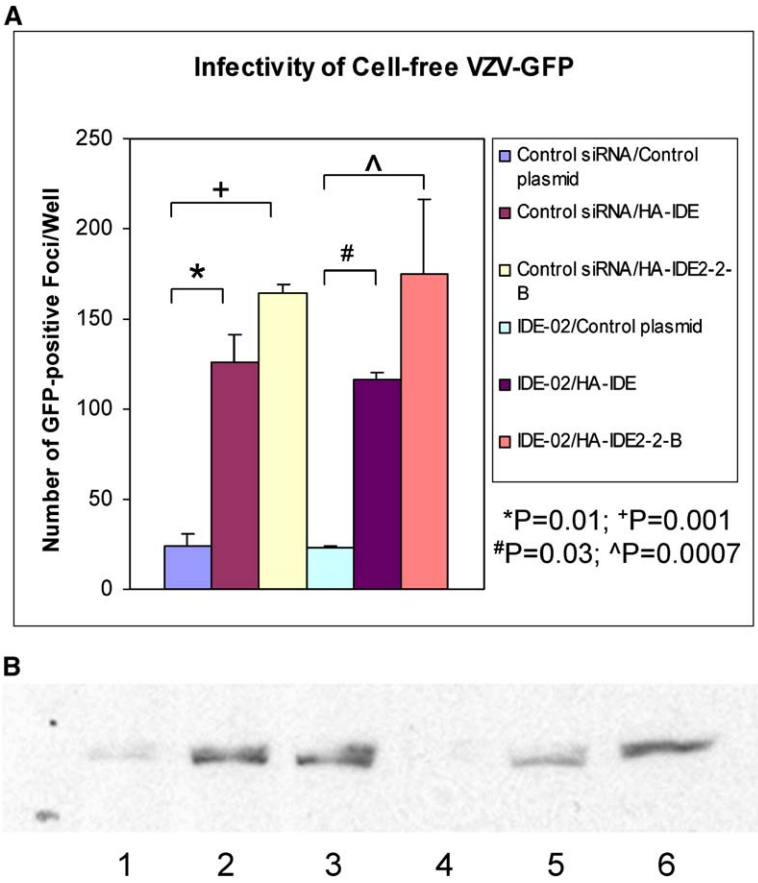

Figure 7. The Level of Human IDE in Cells Correlates with Infectivity by VZV

(A) Transfection of CHO cells with plasmid expressing HA-IDE or human IDE that is resistant to siRNA (HA-IDE 2-2-B) followed by infection with ROka-GFP increases the number of GFP-positive foci in CHO cells.

(B) Autoradiogram of total IDE levels in transfected cells. Transfection of CHO cells with plasmids expressing IDE results in increased levels of total (human plus CHO cells) IDE in CHO cells. Beta-actin, detected with an antibody, was used as a loading control (data not shown).

Error bars show standard deviations, and t test was used to determine p values.

knockdown endogenous human IDE and with a modified plasmid expressing human IDE that should be resistant to the IDE-specific siRNA. Plasmid HA-IDE2-2-B was constructed that encodes an HA epitope-tagged human IDE with an altered nucleotide sequence that does not change the predicted amino acid sequence of IDE but should resist downregulation by siRNA IDE-02. Cotransfection of fibroblasts with siRNA IDE-02 and control plasmid, followed by infection with cell-free ROka-lacZ, resulted in reduced size of foci at 4 days after infection, indicative of impaired cell-to-cell spread, compared with cells cotransfected with control siRNA and control plasmid (Figure 6D, lines 1 and 3). The impairment in cell-to-cell spread was rescued by transfection of cells with plasmid expressing siRNA-resistant IDE (HA-IDE2-2-B) (Figure 6D, lines 3 and 4).

We cotransfected CHO cells with specific siRNA to knockdown endogenous CHO IDE and infected the cells with cell-free ROka-GFP 2 days later. Aliquots of the cells were immunoblotted with anti-IDE Ab to verify the level of IDE protein. Cotransfection of CHO cells with IDE-specific siRNA and a control plasmid resulted in reduced levels of endogenous IDE compared with cotransfection of the cells with control siRNA and control plasmid (Figure 7, lanes 4 versus 1). VZV infectivity in the cells was low. In contrast, cotransfection of CHO cells with control siRNA and either plasmid expressing unmodified (HA-IDE) or modified (HA-IDE2-2-B) IDE resulted in increased levels of IDE and a corresponding increase in VZV infectivity (lanes 2 and 3). Cotransfection of cells with IDE-specific siRNA and unmodified plasmid (HA-IDE) resulted in a modest increase in IDE levels and virus infectivity compared with control siRNA and control plasmid (lanes 1 and 5). In contrast, cotransfection of cells with IDE-specific siRNA and siRNA resistant plasmid (HA-IDE2-2-B) resulted in a more substantial increase in IDE levels and virus infectivity (lane 6). Thus, the level of VZV infectivity generally correlated with the level of IDE expression.

DISCUSSION

Here we show that VZV uses IDE as a receptor for infection with cell-free virus and cell-to-cell spread of virus. While four receptors were identified for HSV, each of these molecules interacts with HSV gD, and VZV lacks a gD homolog. While VZV gE coprecipitated with IDE, HSV gE interacted with IDE much more weakly than its VZV homolog. In addition, while bacitracin blocked IDE and inhibited VZV infection and cell-to-cell spread, the antibiotic did not reduce HSV infection or cell-to-cell spread. Although HSV is closely related to VZV and has many homologous genes, our data suggest that HSV does not use IDE as a receptor. These studies allow us to begin to understand

the mechanism of VZV entry and cell-to-cell spread. They also identify gE as a receptor binding protein and confirm a long-standing belief that gE may play an essential role in VZV infectivity, either by cell-free or by cell-associated virus.

IDE is a member of the zinc metalloproteinase family that was initially implicated in insulin degradation (Duckworth, 1988). It is highly conserved among different species and has the ability to interact with a variety of functionally unrelated ligands that share little homology in their primary amino acid sequences. In addition to insulin, glucagon, insulin-like growth factor II (IGF-II), atrial natriuretic peptide, transforming growth factor-α, and β-amyloid protein are substrates for IDE (Duckworth and Kitabchi, 1974; Farris et al., 2003; Hamel et al., 1997; Misbin and Almira, 1989; Muller et al., 1991). Several other proteins, including epidermal growth factor and IGF-I, bind to IDE but are not hydrolyzed by the enzyme (Duckworth et al., 1998). It has been hypothesized that these IDE ligands possess common conformational motifs for binding to IDE (Kurochkin, 1998).

Several other human viruses also use enzymes as receptors, notably human coronavirus 229E, which uses aminopeptidase N (CD13), and human SARS-associated coronavirus, which uses angiotensin-converting enzyme 2. Aminopeptidase N and angiotensin-converting enzyme 2 are, like IDE, members of the zinc metalloprotease family (Delmas et al., 1992; Li et al., 2003). Interestingly, VZV as well as the two coronaviruses use enzymes as receptors, independent of the activity of the enzyme. Although IDE is predominately a cytosolic protein, it is also present on the plasma membrane (Goldfine et al., 1984; Kuo et al., 1993; Yaso et al., 1987). It localizes to apical or basolateral regions in different tissues (Kuo et al., 1993). A novel isoform of IDE is associated with the surface of differentiated, but not undifferentiated, neurons (Vekrellis et al., 2000). This suggests that IDE may have a role in VZV infection of neurons. IDE is also found in endosomes (Duckworth et al., 1998; Hamel et al., 1991). HSV has recently been shown to enter certain cells by endocytosis in a pH-dependent pathway (Nicola et al., 2003). If VZV is endocytosed in certain cells like HSV, then IDE might allow VZV in endosomes to penetrate into the cytosol. The tissue distribution of IDE is ubiquitous (Kuo et al., 1993), which correlates well with the broad tissue tropism of VZV, especially in vivo.

Our results provide evidence to confirm the important role of gE in VZV-mediated cell-to-cell spread. A naturally occurring VZV mutant with a point mutation in gE shows accelerated cell-to-cell spread in cell culture and in human cells in SCID-hu mice (Santos et al., 2000). HSV gE, which is homologous to the VZV glycoprotein, is necessary for directing egress of virus to the basolateral surface of polarized cells (Collins and Johnson, 2003; Dingwell et al., 1994).

Compared to other human herpes viruses, VZV is unique in that it is transmitted from host to host as airborne virus, yet it disseminates within the hosts by cell-to-cell spread, similar to the pathway used for spread of virus in cell culture (Arvin, 2001). Chen et al. (2004) demonstrated that MPR^{ci} is important for cell-free, but not cell-associated, VZV infection. In contrast, IDE functions as a receptor for both cell-free and cell-associated virus. IDE and MPR^{ci} share some common features. Both molecules interact with some of the same ligands, including IGF-I, IGF-II, and epidermal growth factor (Kuo et al., 1993). At the subcellular level, IDE and MPR^{ci} both localize abundantly in endosomes, a compartment important for VZV trafficking and maturation (Hambleton et al., 2004). Therefore, IDE and MPR^{ci} might interact with each other to facilitate virus infection. Chen et al. (2004) showed that virus maturation was altered in MPR^{ci} -deficient cells, and cell-free virions were released into the medium in cell culture. In contrast, we did not detect a difference in virus maturation by electron microscopy after treatment with an IDE inhibitor (Figure S2), and inhibition of IDE did not result in release of detectable cell-free infectious virus into the cell-culture media (Q.L. and J.C., unpublished data).

Many viruses have evolved to use multiple receptors to augment their infectivity. Two observations from our experiments suggest the possibility that VZV may use more than one receptor. First, blocking IDE resulted in only 25%–75% reduction of VZV infection and cell-to-cell spread. A similar limit on the maximum degree of inhibitory efficiency has been seen with other viruses that use more than one receptor (Akula et al., 2002; Cocchi et al., 1998; Shukla et al., 1999). Second, expression of exogenous human IDE in nonhuman cells rendered them more susceptible to VZV infectivity than to virus binding. It is likely that VZV uses another molecule, in addition to IDE, to bind to cells. Investigations are currently underway to identify other cellular molecules that are important for VZV binding and infection.

In summary, we have identified IDE as a cellular receptor for infection by cell-free and cell-associated VZV. VZV glycoprotein gE, which is essential for virus infection, interacts with IDE through its extracellular domain. Inhibitors of IDE may have a role in the treatment or prevention of VZV infection.

EXPERIMENTAL PROCEDURES

Cells and Viruses

Human fibroblasts (MRC-5), melanoma (MeWo, from C. Grose, University of Iowa), HeLa, CV-1/EBNA (ATCC, Manassas, VA), T (II-23) cells (from C. Ware, La Jolla Institute for Allergy and Immunology) that are susceptible to VZV infection (Zerboni et al., 2000), B78H1 mouse melanoma cells (from N. Fraser, University of Pennsylvania), CHO cells, B3 CHO cells that express human IDE (Vekrellis et al., 2000) (from R. W. Farris, Harvard University), 3T3, and SK-6 A7 cells (from O. Fuller, University of Michigan), were used.

VZV strains ROka (recombinant derived Oka), Molly (a low passage isolate), ROka-lacZ (expressing β-galactosidase) (Cohen et al., 1998), ROka-GFP expressing GFP, or ROka-T7 expressing T7 polymerase (Supplemental Data) were grown in melanoma cells. HSV-1 expressing β-galactosidase was a gift from P. Schaffer (Cai and Schaffer, 1991).

Cell-free virus was prepared by scraping cells from flasks in SPGC buffer (10% fetal bovine serum, 0.1% sodium glutamate, 5% sucrose in PBS), freeze thawing the cells once, sonicating the lysate,

centrifuging the lysate at 1,240× g for 10 min at 4°C, and transferring the supernatant to a new tube for use as cell-free virus.

Antibodies and Reagents

Rabbit polyclonal anti-IDE-1 (provided by R.W. Farris), murine monoclonal anti-IDE 9B12, and rabbit polyclonal anti-IDE antibody, PRB-282C (both from Covance, Berkeley, CA), were used to detect IDE. Soluble IDE protein purified from liver was provided by Dr. R. Bennett (University of Nebraska). Anti-VZV monoclonal antibodies to gE (Chemicon, Temecula, CA), gI, gB (Biodesign, Saco, Maine), and gH (from C. Grose) were used. Bacitracin (Sigma-Aldrich, St. Louis, MO) was dissolved in water. Control Fc fusion proteins including P7.5-Fc (encoding the vaccinia 7.5 protein), were provided by M. Spriggs.

Plasmids

The extracellular domain of gE (amino acids 1–537) was amplified by PCR with SalI and BamHI linkers and inserted into plasmid pDC409 (Giri et al., 1994) to generate plasmid pDC409-gEt. The extracellular domain of gE, along with an in-frame C-terminal human Ig-Fc tag, was cloned into pDC409 to generate plasmid pDC409-gE-Fc. The extracellular domain of gI (amino acids 1–271) was amplified by PCR and cloned into pDC409 to create plasmid pDC409-gIt. PEF6/V5-His-HA-IDE (Vekrellis et al., 2000) encoding HA-tagged human IDE was provided by R.W. Farris. A 3.3 kb (BamHI-NotI) fragment encoding HA-IDE from plasmid pEF6/V5-His-HA-IDE was inserted into baculovirus vector pVL1393 (BD Biosciences Pharmingen, San Diego, CA). Plasmid expressing full-length HSV-2 gE (pcDNA3-gE) was provided by J. Weir (FDA, Bethesda, MD).

Recombinant gE and Biotinylation of Proteins

CV-1/EBNA cells were transfected with plasmids expressing gEt or gE-Fc using Lipofectamine (Invitrogen, Carlsbad, CA) with low Ig FBS (HyClone, Logan, UT). Five days after transfection, tissue culture supernatants were collected. For biotinylation of cell-surface proteins, cell monolayers were incubated with 0.5 mg/ml of EZ-Link Sulfo-NHS-Biotin (Pierce) in PBS (pH8.0) for 30 min at 25°C followed by three washes with cold PBS.

RNA Interference and Ligand Binding Assay

IDE-specific siRNA SmartPools (siRNA-IDE1 and siRNA-IDE2) and two nonspecific control pools (Duplex-13 and C8-scrumple) were synthesized by Dharmacon (Lafayette, CO). Each pool contains four individual siRNA duplex sequences. IDE-specific individual siRNA duplex IDE-02 contains sequence ACACUGAGGUUGCAUAUUUUU (sense sequence). Cells were transfected with 100 nM of individual siRNA or siRNA pools using nucleofection (Amaxa, Gaithersburg, MD).

Histidine (His)-tagged soluble gE and gI (Kimura et al., 1997), gB (R. Williams and S. Straus, personal communication), and HA-tagged IDE were each cloned into baculovirus, and proteins were purified from Sf9-infected cells. HA-IDE protein was coated onto 96-well plates at 4°C for 18 hr. After washing, equal amounts of gEt-His, gIt-His, or gBt-His protein (normalized by ELISA using anti-His antibody) were added and incubated at 4°C for 3 hr. The plates were washed, anti-His-HRP secondary antibody was added, TMB one-step substrate (Dakocytomation, Carpinteria, CA) was added, and binding capacity was detected at OD_{450} nm by an ELISA reader.

Supplemental Data

Supplemental Data include four figures and experimental procedures and can be found with this article online at http://www.cell.com/cgi/content/full/127/2/305/DC1/.

ACKNOWLEDGMENTS

This study was supported by the intramural research program of the National Institute of Allergy and Infectious Diseases. We thank E. Berger, A. Nicola, and S. Straus for reviewing the manuscript. We thank R. Bennett, G. Cohen, R. Farris, N. Fraser, O. Fuller C. Grose, A. Nicola, P. Schaffer, M. Spriggs, S. Straus, W. Studier, C. Ware, J. Weir, and R. Williams for providing reagents.

Received: February 15, 2006
Revised: May 25, 2006
Accepted: August 7, 2006
Published: October 19, 2006

REFERENCES

Akiyama, H., Shii, K., Yokono, K., Yonezawa, K., Sato, S., Watanabe, K., and Baba, S. (1988). Cellular localization of insulin-degrading enzyme in rat liver using monoclonal antibodies specific for this enzyme. Biochem. Biophys. Res. Commun. *155*, 914–922.

Akula, S.M., Pramod, N.P., Wang, F.Z., and Chandran, B. (2002). Integrin alpha3beta1 (CD 49c/29) is a cellular receptor for Kaposi's sarcoma-associated herpesvirus (KSHV/HHV-8) entry into the target cells. Cell *108*, 407–419.

Arvin, A.M. (2001). Varicella-Zoster Virus. In Fields Virology, D.M. Knipe and P.M. Howley, eds. (Philadelphia: Lippincott Williams & Wilkins), pp. 2731–2768.

Bennett, R.G., Hamel, F.G., and Duckworth, W.C. (2003). An insulin-degrading enzyme inhibitor decreases amylin degradation, increases amylin-induced cytotoxicity, and increases amyloid formation in insulinoma cell cultures. Diabetes *52*, 2315–2320.

Cai, W., and Schaffer, P.A. (1991). A cellular function can enhance gene expression and plating efficiency of a mutant defective in the gene for ICP0, a transactivating protein of herpes simplex virus type 1. J. Virol. *65*, 4078–4090.

Chen, J.J., Zhu, Z., Gershon, A.A., and Gershon, M.D. (2004). Mannose 6-phosphate receptor dependence of varicella zoster virus infection in vitro and in the epidermis during varicella and zoster. Cell *119*, 915–926.

Cocchi, F., Menotti, L., Mirandola, P., Lopez, M., and Campadelli-Fiume, G. (1998). The ectodomain of a novel member of the immunoglobulin subfamily related to the poliovirus receptor has the attributes of a bona fide receptor for herpes simplex virus types 1 and 2 in human cells. J. Virol. *72*, 9992–10002.

Cohen, J.I., and Nguyen, H. (1997). Varicella-zoster virus glycoprotein I is essential for growth of virus in Vero cells. J. Virol. *71*, 6913–6920.

Cohen, J.I., and Straus, S. (2001). Varicella-Zoster Virus and its Replication. In Fields Virology, D.M. Knipe and P.M. Howley, eds. (Philadelphia: Lippincott Williams & Wilkins), pp. 2707–2730.

Cohen, J.I., Wang, Y., Nussenblatt, R., Straus, S.E., and Hooks, J.J. (1998). Chronic uveitis in guinea pigs infected with varicella-zoster virus expressing Escherichia coli beta-galactosidase. J. Infect. Dis. *177*, 293–300.

Cole, N.L., and Grose, C. (2003). Membrane fusion mediated by herpesvirus glycoproteins: the paradigm of varicella-zoster virus. Rev. Med. Virol. *13*, 207–222.

Collins, W.J., and Johnson, D.C. (2003). Herpes simplex virus gE/gI expressed in epithelial cells interferes with cell-to-cell spread. J. Virol. *77*, 2686–2695.

Delmas, B., Gelfi, J., L'Haridon, R., Vogel, L.K., Sjostrom, H., Noren, O., and Laude, H. (1992). Aminopeptidase N is a major receptor for the entero-pathogenic coronavirus TGEV. Nature *357*, 417–420.

Dingwell, K.S., and Johnson, D.C. (1998). The herpes simplex virus gE-gI complex facilitates cell-to-cell spread and binds to components of cell junctions. J. Virol. *72*, 8933–8942.

Dingwell, K.S., Brunetti, C.R., Hendricks, R.L., Tang, Q., Tang, M., Rainbow, A.J., and Johnson, D.C. (1994). Herpes simplex virus glycoproteins E and I facilitate cell-to-cell spread in vivo and across junctions of cultured cells. J. Virol. *68*, 834–845.

Duckworth, W.C. (1988). Insulin degradation: mechanisms, products, and significance. Endocr. Rev. *9*, 319–345.

Duckworth, W.C., and Kitabchi, A.E. (1974). Insulin and glucagon degradation by the same enzyme. Diabetes *23*, 536–543.

Duckworth, W.C., Bennett, R.G., and Hamel, F.G. (1998). Insulin degradation: progress and potential. Endocr. Rev. *19*, 608–624.

Farris, W., Mansourian, S., Chang, Y., Lindsley, L., Eckman, E.A., Frosch, M.P., Eckman, C.B., Tanzi, R.E., Selkoe, D.J., and Guenette, S. (2003). Insulin-degrading enzyme regulates the levels of insulin, amyloid beta-protein, and the beta-amyloid precursor protein intracellular domain in vivo. Proc. Natl. Acad. Sci. USA *100*, 4162–4167.

Gabel, C.A., Dubey, L., Steinberg, S.P., Sherman, D., Gershon, M.D., and Gershon, A.A. (1989). Varicella-zoster virus glycoprotein oligosaccharides are phosphorylated during posttranslational maturation. J. Virol. *63*, 4264–4276.

Geraghty, R.J., Krummenacher, C., Cohen, G.H., Eisenberg, R.J., and Spear, P.G. (1998). Entry of alphaherpesviruses mediated by poliovirus receptor-related protein 1 and poliovirus receptor. Science *280*, 1618–1620.

Giri, J.G., Andieh, M., Eisenman, J., Shanebeck, K., Grabstein, K., Kumaki, S., Namen, A., Park, L.S., Cosman, D., and Anderson, D. (1994). Utilization of the beta and gamma chains of the IL-2 receptor by the novel cytokine IL-15. EMBO J. *13*, 2822–2830.

Goldfine, I.D., Williams, J.A., Bailey, A.C., Wong, K.Y., Iwamoto, Y., Yokono, K., Baba, S., and Roth, R.A. (1984). Degradation of insulin by isolated mouse pancreatic acini. Evidence for cell surface protease activity. Diabetes *33*, 64–72.

Hambleton, S., Gershon, M.D., and Gershon, A.A. (2004). The role of the trans-Golgi network in varicella zoster virus biology. Cell. Mol. Life Sci. *61*, 3047–3056.

Hamel, F.G., Gehm, B.D., Rosner, M.R., and Duckworth, W.C. (1997). Identification of the cleavage sites of transforming growth factor alpha by insulin-degrading enzymes. Biochim. Biophys. Acta *1338*, 207–214.

Hamel, F.G., Mahoney, M.J., and Duckworth, W.C. (1991). Degradation of intraendosomal insulin by insulin-degrading enzyme without acidification. Diabetes *40*, 436–443.

Kimura, H., Straus, S.E., and Williams, R.K. (1997). Varicella-zoster virus glycoproteins E and I expressed in insect cells form a heterodimer that requires the N-terminal domain of glycoprotein I. Virology *233*, 382–391.

Kuo, W.L., Montag, A.G., and Rosner, M.R. (1993). Insulin-degrading enzyme is differentially expressed and developmentally regulated in various rat tissues. Endocrinology *132*, 604–611.

Kurochkin, I.V. (1998). Amyloidogenic determinant as a substrate recognition motif of insulin-degrading enzyme. FEBS Lett. *427*, 153–156.

Kwon, H., Bai, Q., Baek, H.J., Felmet, K., Burton, E.A., Goins, W.F., Cohen, J.B., and Glorioso, J.C. (2006). Soluble V domain of Nectin-1/HveC enables entry of herpes simplex virus type 1 (HSV-1) into HSV-resistant cells by binding to viral glycoprotein D. J. Virol. *80*, 138–148.

Li, W., Moore, M.J., Vasilieva, N., Sui, J., Wong, S.K., Berne, M.A., Somasundaran, M., Sullivan, J.L., Luzuriaga, K., Greenough, T.C., et al. (2003). Angiotensin-converting enzyme 2 is a functional receptor for the SARS coronavirus. Nature *426*, 450–454.

Lopez, M., Cocchi, F., Avitabile, E., Leclerc, A., Adelaide, J., Campadelli-Fiume, G., and Dubreuil, P. (2001). Novel, soluble isoform of the herpes simplex virus (HSV) receptor nectin1 (or PRR1-HIgR-HveC) modulates positively and negatively susceptibility to HSV infection. J. Virol. *75*, 5684–5691.

Lowry, P.W., Solem, S., Watson, B.N., Koropchak, C.M., Thackray, H.M., Kinchington, P.R., Ruyechan, W.T., Ling, P., Hay, J., and Arvin, A.M. (1992). Immunity in strain 2 guinea-pigs inoculated with vaccinia virus recombinants expressing varicella-zoster virus glycoproteins I, IV, V or the protein product of the immediate early gene 62. J. Gen. Virol. *73*, 811–819.

Maresova, L., Pasieka, T.J., and Grose, C. (2001). Varicella-zoster Virus gB and gE coexpression, but not gB or gE alone, leads to abundant fusion and syncytium formation equivalent to those from gH and gL coexpression. J. Virol. *75*, 9483–9492.

Misbin, R.I., and Almira, E.C. (1989). Degradation of insulin and insulin-like growth factors by enzyme purified from human erythrocytes. Comparison of degradation products observed with A14- and B26-[125I]monoiodoinsulin. Diabetes *38*, 152–158.

Mo, C., Lee, J., Sommer, M., Grose, C., and Arvin, A.M. (2002). The requirement of varicella zoster virus glycoprotein E (gE) for viral replication and effects of glycoprotein I on gE in melanoma cells. Virology *304*, 176–186.

Montgomery, R.I., Warner, M.S., Lum, B.J., and Spear, P.G. (1996). Herpes simplex virus-1 entry into cells mediated by a novel member of the TNF/NGF receptor family. Cell *87*, 427–436.

Muller, D., Baumeister, H., Buck, F., and Richter, D. (1991). Atrial natriuretic peptide (ANP) is a high-affinity substrate for rat insulin-degrading enzyme. Eur. J. Biochem. *202*, 285–292.

Nicola, A.V., McEvoy, A.M., and Straus, S.E. (2003). Roles for endocytosis and low pH in herpes simplex virus entry into HeLa and Chinese hamster ovary cells. J. Virol. *77*, 5324–5332.

Pertel, P.E., Fridberg, A., Parish, M.L., and Spear, P.G. (2001). Cell fusion induced by herpes simplex virus glycoproteins gB, gD, and gH-gL requires a gD receptor but not necessarily heparan sulfate. Virology *279*, 313–324.

Santos, R.A., Hatfield, C.C., Cole, N.L., Padilla, J.A., Moffat, J.F., Arvin, A.M., Ruyechan, W.T., Hay, J., and Grose, C. (2000). Varicella-zoster virus gE escape mutant VZV-MSP exhibits an accelerated cell-to-cell spread phenotype in both infected cell cultures and SCID-hu mice. Virology *275*, 306–317.

Sattentau, Q.J., and Moore, J.P. (1991). Conformational changes induced in the human immunodeficiency virus envelope glycoprotein by soluble CD4 binding. J. Exp. Med. *174*, 407–415.

Seta, K.A., and Roth, R.A. (1997). Overexpression of insulin degrading enzyme: cellular localization and effects on insulin signaling. Biochem. Biophys. Res. Commun. *231*, 167–171.

Shukla, D., Liu, J., Blaiklock, P., Shworak, N.W., Bai, X., Esko, J.D., Cohen, G.H., Eisenberg, R.J., Rosenberg, R.D., and Spear, P.G. (1999). A novel role for 3-O-sulfated heparan sulfate in herpes simplex virus 1 entry. Cell *99*, 13–22.

Smith, D.H., Byrn, R.A., Marsters, S.A., Gregory, T., Groopman, J.E., and Capon, D.J. (1987). Blocking of HIV-1 infectivity by a soluble, secreted form of the CD4 antigen. Science *238*, 1704–1707.

Vekrellis, K., Ye, Z., Qiu, W.Q., Walsh, D., Hartley, D., Chesneau, V., Rosner, M.R., and Selkoe, D.J. (2000). Neurons regulate extracellular levels of amyloid beta-protein via proteolysis by insulin-degrading enzyme. J. Neurosci. *20*, 1657–1665.

Wu, L., and Forghani, B. (1997). Characterization of neutralizing domains on varicella-zoster virus glycoprotein E defined by monoclonal antibodies. Arch. Virol. *142*, 349–362.

Yaso, S., Yokono, K., Hari, J., Yonezawa, K., Shii, K., and Baba, S. (1987). Possible role of cell surface insulin degrading enzyme in cultured human lymphocytes. Diabetologia *30*, 27–32.

Zerboni, L., Sommer, M., Ware, C.F., and Arvin, A.M. (2000). Varicella-zoster virus infection of a human CD4-positive T-cell line. Virology *270*, 278–285.

Zhu, Z., Gershon, M.D., Ambron, R., Gabel, C., and Gershon, A.A. (1995). Infection of cells by varicella zoster virus: inhibition of viral entry by mannose 6-phosphate and heparin. Proc. Natl. Acad. Sci. USA *92*, 3546–3550.